Published in final edited form as:
Mol Microbiol. 2013 February ; 87(4): 851–866. doi:10.1111/mmi.12136.

CsrA activates *flhDC* expression by protecting *flhDC* mRNA from RNase E-mediated cleavage

Alexander V. Yakhnin[1,3], **Carol S. Baker**[1,3], **Christopher A. Vakulskas**[2], **Helen Yakhnin**[1], **Igor Berezin**[1], **Tony Romeo**[2], and **Paul Babitzke**[1,*]

[1]Department of Biochemistry and Molecular Biology, Center for RNA Molecular Biology, Pennsylvania State University, University Park, PA 16802

[2]Department of Microbiology and Cell Science, PO Box 110700, University of Florida, Gainesville, FL 32611

Summary

Csr is a conserved global regulatory system that controls expression of several hundred *Escherichia coli* genes. CsrA protein represses translation of numerous genes by binding to mRNA and inhibiting ribosome access. CsrA also activates gene expression, although an activation mechanism has not been reported. CsrA activates *flhDC* expression, encoding the master regulator of flagellum biosynthesis and chemotaxis, by stabilizing the mRNA. Computer modeling, gel mobility shift, and footprint analyses identified two CsrA binding sites extending from positions 1–12 (BS1) and 44–55 (BS2) of the 198-nt *flhDC* leader transcript. *flhD'-'lacZ* expression was reduced by mutations in *csrA* and/or the CsrA binding sites. The position of BS1 suggested that bound CsrA might inhibit 5' end-dependent RNase E cleavage of *flhDC* mRNA. Consistent with this hypothesis, CsrA protected *flhDC* leader RNA from RNase E cleavage *in vitro* and protection depended on BS1 and BS2. Primer extension studies identified *flhDC* decay intermediates *in vivo* that correspond to *in vitro* RNase E cleavage sites. Deletion of these RNase E cleavage sites resulted in increased *flhD'-'lacZ* expression. Data from mRNA decay studies and quantitative primer extension assays support a model in which bound CsrA activates *flhDC* expression by inhibiting the 5' end-dependent RNase E cleavage pathway.

Keywords

CsrA; RNase E; mRNA stability; gene regulation; motility; RNA binding protein

Introduction

Csr (carbon storage regulator) is a conserved global regulatory system that potentially regulates expression of several hundred genes in *Escherichia coli* (Edwards *et al.*, 2011). The Csr system, also called Rsm (repressor of secondary metabolites) in some organisms, regulates virulence factors, quorum sensing, motility, carbon metabolism, peptide uptake, and biofilm development in various eubacterial species (reviewed in Babitzke and Romeo, 2007; Romeo *et al.*, 2012). The major components of the *E. coli* Csr system include the homodimeric RNA binding protein CsrA (Liu and Romeo, 1997), two noncoding small RNAs (sRNA) CsrB and CsrC (Liu *et al.*, 1997; Weilbacher *et al.,* 2003), the BarA-UvrY two-component signal transduction system (TCS) that activates *csrB* and *csrC* transcription (Suzuki *et al.,* 2002; Weilbacher *et al.,* 2003), and CsrD, a protein that participates in RNase

*Corresponding author Phone: 814-865-0002 Fax: 814-863-7024 pxb28@psu.edu.
[3]These authors contributed equally to the work.

E-mediated degradation of the sRNAs (Suzuki *et al.,* 2006). CsrB and CsrC contain several CsrA binding sites and antagonize CsrA binding to mRNA targets (Liu *et al.*, 1997; Weilbacher *et al.,* 2003; Babitzke and Romeo, 2007; Romeo *et al.*, 2012).

Regulation of the *E. coli* Csr system is complex. Transcription of *csrA* is controlled by five promoters, two of which are σ^S-dependent. CsrA also indirectly activates its own transcription (Yakhnin *et al.,* 2011a). The Csr system is also controlled by three negative feedback loops. In one case CsrA represses expression of CsrD, thereby stabilizing its own sRNA antagonists (Suzuki *et al.,* 2006). In another regulatory loop CsrA indirectly stimulates transcription of *csrB* and *csrC* via the BarA-UvrY TCS, which responds to acetate and other short chain fatty acids (Suzuki *et al.,* 2002; Chavez *et al.,* 2010). Finally, CsrA represses its own translation, thereby ensuring that CsrA levels are tightly controlled (Yakhnin *et al.,* 2011a).

CsrA represses translation initiation of a variety of genes, typically by binding to multiple sites in the leader region of target mRNAs, one of which overlaps the cognate Shine-Dalgarno (SD) sequence, such that bound CsrA blocks 30S ribosomal subunit binding (Babitzke and Romeo, 2007; Edwards *et al.*, 2011; Yakhnin *et al.,* 2011a; Pannuri *et al.,* 2012). However, CsrA represses translation of *hfq* by binding to a single site that overlaps its SD sequence (Baker *et al.,* 2007), as well as *sdiA* by binding exclusively to two sites in the amino terminal coding region (Yakhnin *et al.,* 2011b). Translational repression often leads to rapid mRNA decay (Babitzke and Romeo, 2007). CsrA is a homodimer with two identical RNA-binding surfaces that simultaneously bind two sites within a transcript (Dubey *et al.*, 2003; Mercante *et al.,* 2006; 2009). Considerable sequence variation exists among the known CsrA binding sites; however, GGA is a highly conserved motif that is often present in the loop of short RNA hairpins (Dubey *et al.*, 2005; Babitzke and Romeo, 2007).

RNase E is an essential endonuclease that cleaves RNA in single-stranded AU-rich regions (McDowall *et al.,* 1994). This enzyme plays a central role in the degradation of mRNA and in a variety of RNA processing reactions (Kime *et al.,* 2008; Steade *et al.*, 2011). RNase E cleavage can occur by a 5' end-dependent mechanism in which 5' monophosphorylated transcripts interact with a 5' binding pocket on the enzyme (Callaghan *et al.,* 2005). In addition to the 5' end-dependent pathway, RNase E is capable of cleaving transcripts by an internal entry pathway that does not involve interaction with the 5' end of the transcript (Mackie, 1998; Kime *et al.,* 2010). When translation of mRNA is inhibited, transcripts are generally more susceptible to degradation by RNase E (Richards *et al.,* 2012). The single-stranded RNA cleavage activity of RNase E is located in the N-terminal domain of the enzyme (Callaghan *et al.,* 2005). Although the C-terminal domain of RNase E is not essential (Ow *et al.,* 2000), it serves as a scaffold for assembly of a multisubunit complex called the degradosome, which also includes a processive 3' to 5' exoribonuclease (polynucleotide phosphorylase, PNPase), an RNA helicase (RhlB), and enolase. RNase E and PNPase can function independently, but association with the degradosome may coordinate RNA decay (reviewed in Carpousis, 2007; Arraiano *et al.,* 2010). The composition and function of the degradosome may be altered by environmental conditions and modulated by other proteins including RraA and RraB, which inhibit RNase E activity (Gao *et al.,* 2006; Carpousis, 2007).

Although CsrA-mediated translational repression is well documented, a molecular mechanism of CsrA-mediated activation has not been identified. CsrA activates expression of the *flhDC* operon (Wei *et al.,* 2001), encoding a hexameric DNA binding protein ($FlhD_4C_2$) (Wang *et al.,* 2006). $FlhD_4C_2$ plays a key role in activating flagellum synthesis and chemotaxis (reviewed in Smith and Hoover, 2009). Transcriptional regulation of *flhDC*

expression occurs in response to many environmental factors including changes in temperature, osmolarity, pH, and the availability of carbon sources (Smith and Hoover, 2009). Examination of growth phase regulation of *flhDC* demonstrated that protein levels were highest at mid-exponential phase with a second peak occurring during the transition to stationary phase (Prüß and Matsumura, 1997). Previous results demonstrated that CsrA increases *flhDC* expression by stabilizing the transcript, although the underlying mechanism was not investigated (Wei *et al.,* 2001). Here, we explored the mechanism of CsrA-mediated activation of *flhDC* expression. Two CsrA binding sites were identified in the *flhDC* leader transcript that are required for CsrA-dependent activation of *flhDC* expression. Our data further indicate that CsrA binding to these two sites stabilizes the *flhDC* transcript by interfering with the 5' end-dependent RNase E cleavage pathway.

Results

CsrA binds to two sites in the flhDC leader transcript

We previously found that expression of a *flhDC'-'lacZ* translational fusion was reduced in a *csrA::kan* strain, which correlated with a reduction in the *flhDC* mRNA half-life (Wei *et al.*, 2001). In addition, *csrA* mutant cells were non-motile and lacked flagella (Wei *et al.*, 2001). A 198-nt untranslated leader precedes the *flhD* coding sequence. RNA structure predictions using Mfold (Zuker, 2003) suggested that the *flhDC* untranslated leader was highly structured. Results from RNA structure mapping experiments using RNase T_1 as a probe (single-stranded G specific) were consistent with five hairpin structures (HP1-HP5) that form in the leader transcript (Fig. 1A, 1B and 1C [0 μM CsrA]). As HP5 includes the *flhD* SD sequence in the loop of the structure, we tested whether bound CsrA altered the structure in such a way that the SD sequence would be more accessible for 30S ribosomal subunit binding, thereby providing an explanation for CsrA-mediated gene activation. The RNase T_1 cleavage pattern of the G residues between positions 109 and 240, which includes the *flhD* SD sequence, was unaffected by bound CsrA; however, we did observe CsrA-dependent protection of G residues in the loops of HP1 and HP2 (Fig. 1C, 1 μM CsrA).

A position weighted matrix search tool (Baker *et al.*, 2007) identified two potential CsrA binding sites in the first 55 nt of the *flhDC* leader transcript, both of which contained the conserved GGA motif (Fig. 1A). Importantly, these two predicted binding sites contained the protected G residues in the loops of HP1 and HP2 (Fig. 1B and 1C). To provide further evidence for CsrA binding in this region, footprint experiments were conducted with a transcript containing residues 1–99. CsrA protected each of the G residues in binding sites 1 and 2 (BS1 and BS2) from RNase T_1 cleavage, but did not protect any of the other G residues. CsrA also protected several nucleotides in BS1 and BS2 from cleavage by RNase T_2 (single-stranded A preference) (Fig. 1A, 1B and 1D). The cleavage pattern of A residues in BS1 suggests that bound CsrA protects HP1 directly by binding to the single stranded loop, and perhaps indirectly by stabilizing the hairpin structure (Schubert *et al.*, 2007). HP2 was maintained in the presence or absence of CsrA. Thus, the footprinting results confirm that CsrA binds to both predicted sites. Furthermore, the footprinting data indicate that bound CsrA does not bind to nor does it alter the RNA structure in the region surrounding the *flhD* ribosome binding site (Fig. 1C), suggesting that CsrA may not affect translation of *flhD*.

Gel mobility shift assays were performed to characterize the interaction of CsrA with the same 99-nt RNA used in the footprinting experiments. CsrA bound to this transcript as a diffuse band between 1 and 32 nM CsrA, with a distinct band becoming prominent at the higher concentrations (Fig. 2). Quantification of these data yielded an apparent K_d value of 21 nM CsrA. Deletion of the GGA motif from BS1 (ΔBS1) resulted in a 5-fold decrease in binding affinity, whereas deletion of the GGA from BS2 (ΔBS2) resulted in a 20-fold

binding defect. Importantly, deletion of both GGA motifs virtually eliminated CsrA binding (Fig. 2). The specificity of CsrA-*flhDC* leader RNA interaction was investigated by performing competition experiments with specific (*flhD* and *pgaA*) and non-specific RNA competitors (Fig. 2). Unlabeled *E. coli flhD* and *pgaA* were effective competitors for CsrA-*flhD* RNA interaction, whereas only minimal competition was observed with RNA derived from pTZ19R vector sequences, demonstrating that CsrA binds specifically to *flhDC* leader RNA.

Loss of CsrA binding to the flhDC leader transcript reduces flhDC expression

A *csrA* deletion was shown to be viable in a strain containing a mutation in the glycogen biosynthetic operon (*glg*) (Timmermans and Van Melderen, 2009). We constructed a similar strain and found that it grew poorly and appeared to acquire suppressor mutations. For this reason, we used a well-characterized *csrA* mutant allele (*csrA::kan*) containing a transposon insertion following the 50th codon in the 61 aa coding sequence (Romeo *et al.* 1993).

As CsrA binds to two sites in *flhDC* leader RNA, we tested the effect of *csrA* on expression of a plasmid-borne *flhDC'-'lacZ* translational fusion. Expression peaked in late exponential phase growth and was reduced in the *csrA* mutant (Fig. 3A), consistent with our previous finding that CsrA activates *flhDC* expression (Wei *et al.* 2001). Expression of a chromosomally integrated *flhD'-'lacZ* translational fusion was also tested. Although expression of this single-copy *flhD'-'lacZ* fusion was 4- to 5-fold lower than the plasmid-borne *flhDC'-'lacZ* fusion (Fig. 3B), expression of the integrated *flhD'-'lacZ* fusion was reduced in the *csrA* mutant to a similar extent as was observed for the plasmid-borne *flhDC'-'lacZ* fusion, indicating that CsrA-dependent activation of *flhDC* expression is unaffected by the *flhDC* copy number. We next tested the effect of the ΔBS1 and/or ΔBS2 mutations on expression of chromosomally integrated *flhD'-'lacZ* translational fusions in wild type (WT) and *csrA* mutant strains. Expression in the WT strain was reduced when the fusion carried a mutation in either BS1 or BS2, while mutating both binding sites resulted in a further reduction in expression (Fig. 3C). Expression levels in the *csrA* mutant background were similar for the WT, BS1 and BS2 mutant fusions, while expression was reduced when both binding sites were mutated (Fig. 3D).

The results in figure 3D were somewhat surprising because we did not expect that mutating the CsrA binding sites would cause a further reduction in expression in the *csrA* mutant. However, the mutant *csrA* allele contains a transposon insertion following the 50th codon in the 61 aa coding sequence, resulting in a 62 aa fusion protein. As L2, L4, R6, R7, V40, V42, R44 and I47 are critical for RNA interaction (Mercante *et al.*, 2006), it was possible that the fusion protein retained some RNA binding activity. Thus, the mutant fusion protein was purified, and its activity was assessed using a 16-mer RNA target containing a single high-affinity CsrA binding site (Dubey *et al.*, 2005; Mercante *et al.*, 2009). Gel mobility shift results confirmed that the fusion protein retained significant binding activity; the binding affinity of the fusion protein was reduced 8-fold compared to WT CsrA (Fig. 4). Perhaps the reduction in *flhD'-'lacZ* expression caused by mutating BS1 and BS2 in the *csrA::kan* genetic background is explained by the partial RNA binding activity of the fusion protein.

Bound CsrA protects flhDC leader RNA from RNase E-mediated cleavage in vitro

The positions of BS1 and BS2, combined with the observation that bound CsrA does not cause structural rearrangements of *flhDC* leader RNA, suggested that the mechanism of *flhDC* activation and mRNA stabilization was restricted to the 5' end of the message. As RNase E possesses a 5' end-dependent cleavage mechanism with a strong preference for 5' monophosphorylated RNAs (Mackie, 1998; Kime *et al.*, 2010), we hypothesized that bound CsrA could sequester the 5' end of *flhDC* leader RNA and inhibit RNase E-mediated

cleavage. To test this hypothesis, 5' monophosphorylated RNAs containing WT or ΔBS1 ΔBS2 leaders were incubated with purified RNase E *in vitro*. In the absence of CsrA, cleavage occurred primarily between nucleotides 100 and 120, although minor cuts were also observed within BS2 and near position 145 (Fig. 1B and 5A). Note that the different sized cleavage products between the WT and mutant transcripts reflect the GGA deletions in BS1 and BS2. The cleavage sites between positions 100 and 120 were at the same nucleotides for both transcripts; however, there were qualitative differences in the cleavage pattern. Bound CsrA protected WT RNA from cleavage in the 100–120 and BS2 regions, the latter of which served as an internal control for CsrA binding. Importantly, CsrA-dependent protection from RNase E cleavage was eliminated in the ΔBS1 ΔBS2 RNA (Fig. 5A).

Although RNase E exhibits a preference for 5' monophosphorylated RNA, cleavage can occur by an internal entry pathway in which the 5' end is bypassed (Mackie, 1998; Kime *et al.*, 2010). Thus, we performed RNase E assays with *flhDC* leader transcripts that were labeled at the 3' end such that they retained 5' triphosphates and found that the cleavage rate was about 8-fold slower compared to 5' monophosphorylated RNA (data not shown). We also determined the effects of CsrA on RNase E cleavage of WT and ΔBS1 ΔBS2 RNAs containing 5' triphosphates. In this case CsrA-dependent protection of the WT transcript was greatly reduced relative to RNA containing a 5' monophosphate (Fig. 5B). As for the 5' monophosphorylated substrate, CsrA did not protect the ΔBS1 ΔBS2 transcript containing a 5' triphosphate. We conclude that bound CsrA protects the *flhDC* leader transcript by interfering with the 5' end-dependent RNase E cleavage pathway *in vitro*.

Bound CsrA stabilizes flhDC mRNA in vivo

As bound CsrA inhibits RNase E-mediated cleavage of the *flhDC* leader transcript *in vitro*, mRNA half-life experiments were conducted to examine the effect of CsrA on *flhDC* mRNA stability *in vivo*. Since we were unable to detect the *flhDC* transcript expressed from its native chromosomal locus by Northern blotting, experiments were performed with strains containing plasmids pCSB81 (WT *flhDC* operon) or pCSB83 (ΔBS1 ΔBS2 *flhDC* operon). Recall that the extent of CsrA-dependent activation of *flhDC* expression was unaffected by the *flhDC* copy number (Fig. 3). The influence of CsrA and the CsrA binding sites on the rate of *flhDC* mRNA decay was examined at 30°C, the same growth temperature used for the expression studies (Fig. 3). The half-life of the WT transcript was ~1 min in the WT strain and ~0.5 min in the *csrA* mutant strain. Importantly, the half-life of the ΔBS1 ΔBS2 *flhDC* transcript was ~0.5 min in both WT and *csrA* strains (Fig. 6). Recall that CsrA is unable to bind to this RNA (Fig. 2). We conclude that bound CsrA stabilizes the *flhDC* transcript twofold, which is similar to its threefold effect on expression of the *flhD'-'lacZ* fusion (Fig. 3).

As described above, RNase E preferentially acts on RNA containing a 5' monophosphate (Mackie, 1998). Since *E. coli* RppH is the 5' pyrophosphatase that converts 5' triphosphates to 5' monophosphates (Deana *et al.*, 2008), we examined the effect of RppH on the stability of WT and ΔBS1 ΔBS2 *flhDC* transcripts. While the absence of RppH did not affect the stability of the WT transcript, the ΔBS1 ΔBS2 transcript was stabilized twofold in the absence of RppH (Fig. 6). We conclude that a 5' triphosphate can substitute for bound CsrA in stabilizing *flhDC* mRNA *in vivo*, which is consistent with bound CsrA interfering with the 5' end-dependent RNase E cleavage pathway.

As a test of this hypothesis, we compared expression levels of the WT and ΔBS1 ΔBS2 *flhD'-'lacZ* fusions in WT and *rppH* mutant strains. However, rather than the expected increase in expression, the absence of RppH caused a small decrease in expression of both fusions (data not shown). Because *flhDC* expression is activated and repressed by a variety

of transcription factors (Shin *et al.*, 1995; Soutourina *et al.*, 1999; Lehnen *et al.*, 2002; Sperandio *et al.*, 2002; Smith and Hoover, 2009), while RppH affects the turnover of bulk mRNA, it is likely that the decrease in expression is due to indirect effects of RppH-deficiency on one or more of these transcription factors.

Deletion of the RNase E cleavage sites from the flhDC leader increases expression of the flhDC operon

Results from the *in vitro* RNase E cleavage and *in vivo* Northern analyses are consistent with bound CsrA protecting the *flhDC* leader transcript from cleavage between positions 100 and 120 (Figs. 5 and 6). Thus, primer extension mapping was used to determine if the leader transcript is cleaved in the same region *in vivo*. Each strain used in this analysis contained the *pnp-200* and *rnb-500* alleles, which encode thermolabile PNPase and RNase II, respectively. Use of this genetic background leads to stabilization of endonucleolytic cleavage intermediates after a shift to the non-permissive temperature by inactivating two exonucleases that play important roles in mRNA turnover (Yancey and Kushner, 1990; Arraiano *et al.,* 2010). In addition, one of the strains contained the *rne-1* allele, encoding thermolabile RNase E (Babitzke and Kushner, 1991). Several primer extension products were reduced or absent in the *rne-1* strain following a shift to 44°C (Fig. 7). Five of the prominent bands (101, 113, 116, 142 and 145) correspond to RNase E cleavage sites that were observed *in vitro*. Moreover, CsrA protected positions 101, 113 and 116 from RNase E cleavage *in vitro* (Fig. 5). We conclude that RNase E cleaves *flhDC* leader RNA *in vivo* at some of the sites that CsrA protected from RNase E cleavage *in vitro*. We also examined the effect of CsrA on cleavage at these sites *in vivo*; however, the accumulation of cleavage intermediates was unaffected by CsrA deficiency or overexpression (data not shown).

The data presented above provided compelling evidence that bound CsrA activates *flhDC* expression by protecting the mRNA from the 5' end-dependent RNase E cleavage pathway. As an additional test of this model, we deleted residues +97 through +122 from the *flhDC* leader, as the majority of the *in vitro* RNase E cleavage sites are within this region (Fig. 1B and 5). Deletion of this region eliminated RNase E cleavage between BS2 and positions 142 and 145 *in vitro* (Fig. 8A). We then compared expression of an integrated Δ97-122 (ΔE) *flhD'-'lacZ* fusion to WT and ΔBS1 ΔBS2 *flhD'-'lacZ* fusions. Consistent with CsrA-mediated protection of the region between 100 and 120 from RNase E cleavage *in vitro*, the ΔE fusion resulted in a substantial increase in expression (Fig. 8B). This result is consistent with a model in which CsrA-dependent protection from RNase E cleavage leads to increased expression of the *flhDC* operon. We next compared expression of the WT and ΔE fusions in WT and *csrA* mutant strains. Introduction of the *csrA* allele reduced expression of the ΔE fusion, but not to the level of the WT fusion (Fig. 8C). These latter results suggest that CsrA is still capable of protecting the *flhDC* transcript from cleavage at RNase E sites that remain in the ΔE fusion and/or from an alternative mRNA decay pathway.

Our primer extension mapping experiments identified RNase E-dependent degradation intermediates, some of which arose from cleavage at sites that were protected from RNase E cleavage by bound CsrA *in vitro* (Figs. 5 and 7). To obtain direct evidence of CsrA-dependent protection of the *flhDC* leader transcript from RNase E cleavage *in vivo*, we carried out quantitative primer extension assays using a *lacZ*-specific primer and RNA purified from strains with integrated WT, ΔBS1 ΔBS2 (ΔBS), ΔE, or ΔBS ΔE *flhD'-'lacZ* fusions. Each fusion was tested in WT and *rne-1* genetic backgrounds before and after a shift to the non-permissive temperature (44°C). Thus, the level of a full-length primer extension product would reflect the effects of bound CsrA and/or RNase E on *flhDC* mRNA turnover. The level of a primer extension product corresponding to tmRNA was used as an internal loading control for each sample; the level of tmRNA was not affected by the ΔBS, ΔE, or *rne-1* mutations.

The shift to 44°C resulted in rapid degradation of the WT transcript in the WT (*rne+*) background but not in the *rne-1* strain, which encoded thermolabile RNase E (Fig. 9A, first four lanes). Rapid degradation of *flhDC* mRNA at 44°C is consistent with a severe motility defect at this temperature (data not shown). The stability of the ΔBS transcript was twofold lower than the WT transcript in the *rne+* genetic background at both temperatures (Fig. 9A). Importantly, the twofold reduction in transcript stability caused by loss of CsrA binding was essentially identical to what was previously observed in the Northern studies (Fig. 6). Of particular interest, the stability of the ΔBS transcript in the *rne-1* strain at 44°C was similar to its stability in the *rne+* strain at 30°C, indicating that destabilization of the *flhDC* transcript caused by the loss of CsrA binding was overcome when RNase E was inactivated (Fig. 9A). Compared to the WT and ΔBS transcripts, deletion of the RNase E sites from the *flhDC* leader (ΔE) led to considerable stabilization of the transcript in the *rne+* background at 44°C (Fig. 9A), confirming that this region is normally cleaved by RNase E *in vivo*. Decay of the ΔBS ΔE transcript was intermediate between the ΔBS and ΔE transcripts. This latter finding suggests that bound CsrA protects the *flhDC* transcript from cleavage at sites in addition to those removed by the ΔE mutation. From the results of these experiments we conclude that bound CsrA protects the *flhDC* leader transcript from RNase E cleavage *in vitro* and *in vivo*.

It is well established that increasing or decreasing translation can lead to mRNA stabilization or destabilization, respectively (e.g. Babitzke and Romeo, 2007; Arraiano *et al.*, 2010; Richards *et al.,* 2012). Although the CsrA binding sites are about 190 (BS1) and 150 (BS2) nt upstream of the *flhD* translation initiation codon, while bound CsrA did not affect the *flhDC* leader RNA structure in the vicinity of the *flhD* SD sequence (Fig. 1), we had not ruled out the possibility that CsrA-dependent protection of the *flhDC* transcript is an indirect effect of CsrA-mediated translational activation. To test this possibility we performed quantitative primer extension studies using a *flhDC* leader-specific primer and RNA purified from strains with integrated WT, ΔBS, ΔE and ΔBS ΔE constructs in which the *flhDC* leader sequence downstream from position 146 was replaced with the strong λtR_2 intrinsic terminator (Fig. 1B and 9B). Since none of these transcripts can be translated, any observed effect on RNA stability would be independent of translation. Decay of the WT, ΔBS and ΔE transcripts was similar to those observed for the corresponding translational fusion transcripts (Fig. 9A and 9B). Thus, we conclude that CsrA-dependent protection of *flhDC* mRNA from RNase E cleavage is independent of translation. A notable difference in the decay of these transcripts was observed after the shift to 44°C; stabilization due to RNase E deficiency (*rne-1*) was less pronounced than for the corresponding fusion transcripts. In contrast to the other three transcripts, decay of the ΔBS ΔE transcript was much more rapid (Fig. 9B), indicating that this transcript can be degraded by an alternative decay pathway (see Discussion).

Discussion

CsrA is a widely distributed global regulatory protein that binds to several hundred different *E. coli* transcripts (Edwards *et al.*, 2011). A variety of related CsrA-mediated translation repression mechanisms have been identified in which CsrA binds near the translation initiation region and/or SD sequence of target transcripts, thereby blocking 30S ribosomal subunit binding (Babitzke and Romeo, 2007). Despite evidence for activation of several genes in *E. coli* (Sabnis *et al.*, 1995; Wei *et al.*, 2001), until now a CsrA-mediated activation mechanism had not been identified. We found that CsrA activates *flhDC* operon expression by binding to two sites in the leader transcript that are separated by 31 nt (Fig. 1–3). The level of activation is similar in magnitude to the level of CsrA-dependent stabilization of the *flhDC* transcript (Fig. 3, 6 and 9). The finding that the mutant CsrA fusion protein encoded by the *csrA::kan* allele retained significant RNA binding activity (Fig. 4) suggests that the

reported level of CsrA-mediated regulation for all CsrA-controlled genes in *E. coli* is underrepresented.

CsrA binding to the extreme 5' end of *flhDC* mRNA led to the hypothesis that sequestration of the 5' end by bound CsrA would inhibit 5' end-dependent cleavage by RNase E. Computer modeling and *in vitro* structure mapping revealed five hairpins (HP1-HP5) that likely form in the leader region of *flhDC* RNA (Fig. 1). The GGA motifs of BS1 and BS2 are located in the loops of HP1 and HP2, a common sequence arrangement of CsrA binding sites (Liu *et al.*, 1997; Weilbacher *et al.*, 2003; Dubey *et al.*, 2005; Babitzke and Romeo, 2007). The predominant RNase E cleavage sites between positions 100 and 120 are located in an AU-rich region just downstream from HP2 (Fig. 5), a sequence arrangement that is similar to RNase E recognition sites found in other mRNA substrates (Carpousis, 2007; Kime *et al.*, 2008). Deletion of the prominent RNase E cleavage sites between +97 to +122 (ΔE) resulted in increased *flhD'-'lacZ* expression (Fig. 8) and mRNA stabilization (Fig. 9). Furthermore, three of the *flhDC* decay intermediates that were identified *in vivo* by primer extension correspond to RNase E cleavage sites that CsrA protected from cleavage *in vitro* (Fig. 5 and 7). In conjunction with the finding that bound CsrA stabilizes the *flhDC* transcript (Fig. 6 and 9), we conclude that CsrA activates *flhDC* expression by protecting *flhDC* mRNA from endonucleolytic cleavage by RNase E.

Degradation of several mRNAs depends on a rate-limiting cleavage event by RNase E, resulting in a new 3' end that is degraded by 3' to 5' exonucleases (reviewed in Carpousis, 2007; Arraiano *et al.*, 2010). RNase E cleavage also results in a new 5' monophosphorylated end that serves as a preferred RNase E substrate for cleavage further downstream (Deana *et al.*, 2008). Thus sequential RNase E-mediated cleavage events, followed by exonucleolytic digestion of the resulting fragments from the 3' end, is thought to be a common mechanism for mRNA turnover in *E. coli* (Carpousis, 2007; Arraiano *et al.*, 2010). RNase E cleaved several residues between positions 100 and 120 of the *flhDC* leader transcript that could serve as a rate-limiting cleavage event *in vivo*. RppH is responsible for converting the 5' terminal triphosphate to a monophosphate *in vivo* (Deana *et al.*, 2008). Because RNase E has a preference for 5' monophosphate ends, the findings that a 5' triphosphate can compensate for bound CsrA in stabilizing the *flhDC* transcript *in vitro* (Fig. 5B) and *in vivo* (Fig. 6), indicate that bound CsrA protects the *flhDC* transcript from the 5' end-dependent RNase E cleavage pathway. In this mechanism, CsrA binding at BS1 would sequester the 5' end of the mRNA, thereby inhibiting RNase E action. CsrA bound at BS2 probably increases the affinity of CsrA interaction with the weaker BS1 due to its ability to bridge two RNA binding sites (Mercante *et al.*, 2009). Our studies further imply that CsrA-mediated stabilization of the *flhDC* transcript leads to increased $FlhD_4C_2$ synthesis, which, in turn, activates flagellum synthesis and cell motility.

A recently published paper identified a 95 nt sRNA (McaS). This sRNA is expressed during late exponential and early stationary phase growth (Thomason *et al.*, 2012). McaS is capable of activating *flhDC* expression ~1.4-fold by hybridizing to two sites in the *flhDC* leader transcript (positions 113 to 122 and 138 to 147, Fig. 1B). It was suggested that McaS might alter a predicted long-range RNA structure that sequesters the SD sequence, thereby relieving translational repression (Thomason *et al.*, 2012). However, our structure mapping results are incompatible with this long-range structure and instead support the formation of five RNA hairpins (Fig. 1). In light of our data presented here, we offer an alternative hypothesis for the mechanism of McaS action. The upstream McaS hybridization site (McaS BS1) partially overlaps the RNase E cleavage sites between positions 100 and 120, while the downstream McaS hybridization site (McaS BS2) overlaps the RNase E cleavage sites at positions 142 and 145 (Fig. 1B). Thus the mechanism of McaS-mediated activation may involve protection of the *flhDC* leader from RNase E cleavage. Since our primer extension

studies were performed with cultures grown to late exponential phase, this mechanism may explain the rapid decay observed for the ΔBS ΔE transcript (Fig. 9B). Deletion of the RNase E cleavage sites between positions 100 and 120 eliminated McaS BS1, while the engineered tR_2 terminator sequesters the 3' end of McaS BS2. Thus, McaS may not interact with this transcript. Perhaps the lack of CsrA and McaS binding to this ΔBS ΔE transcript results in rapid RNA turnover. Note that all of the other transcripts described in figure 9 contained the CsrA binding sites and/or at least one of the McaS binding targets. While our results demonstrate that CsrA protects the *flhDC* transcript from the 5' end-dependent RNase E cleavage pathway, future studies will be required to identify the mechanism of McaS action and any potential connection with CsrA-dependent activation of *flhDC* expression.

Experimental procedures

Plasmids

The cloning vector pBR322 (Bolivar *et al.*, 1977), the CRIM-based translational (pLFT) and transcriptional (pLFX) fusion vectors (Edwards *et al.*, 2011), and pFDCZ6 containing a WT *flhDC'-'lacZ* translational fusion (Wei *et al.*, 2001) have been described. Deletions of the GGA motifs from CsrA binding sites BS1 [G7, G8, A9 (ΔBS1)] and/or BS2 [G50, G51, A52 (ΔBS2)] were introduced into the *flhDC* leader in pFDCZ6 using the QuikChange protocol (Stratagene), resulting in plasmids, pCSB74 (ΔBS1), pCSB72 (ΔBS2) and pCSB75 (ΔBS1 ΔBS2). *flhD'-'lacZ* translational fusions were generated by PCR amplification of *flhDC* sequences extending from − 195 to +234 relative to the start of transcription using pFDCZ6, pCSB74, pCSB72 and pCSB75 as templates. The PCR products were digested with PstI and EcoRI and cloned into the same sites of pLFT. The resulting plasmids, pCSB76 (WT *flhD'-'lacZ*), pCSB77 (ΔBS1 *flhD'-'lacZ*), pCSB78 (ΔBS2 *flhD'-'lacZ*) and pCSB79 (ΔBS1 ΔBS2 *flhD'-'lacZ*), have the 12^{th} codon of *flhD* fused in frame to the 10^{th} codon of *lacZ*. Deletion of the RNase E cleavage sites between +97 and +122 (ΔE) was accomplished by the QuikChange protocol using pCSB76 and pCSB79 as DNA templates, resulting in plasmids pAY144 (ΔE *flhD'-'lacZ*) and pYH203 (ΔBS1 ΔBS2 ΔE *flhD'-'lacZ*), respectively. Plasmid pCSB81 contains the entire *flhDC* operon cloned into the BamHI and EcoRI sites of pBR322. Deletion of the GGA motifs from CsrA binding sites BS1 and BS2 were introduced into the *flhDC* leader in pCSB81 using the QuikChange protocol, resulting in plasmid pCSB83.

Plasmids with the *flhDC* promoter and a truncated leader region (−195 to +146 relative to the start of transcription) in which sequences downstream from +146 were replaced by the λtR_2 intrinsic terminator were constructed as follows. PCR amplification of WT and mutant *flhDC* leader fragments followed by λtR_2 was accomplished using plasmids pCSB76, pCSB79, pAY144 and pYH203 as DNA templates. The downstream primer in these reactions contained the λtR_2 sequence. The resulting PCR products were digested with EcoRI and PstI and cloned into the same sites of pLFX, resulting in plasmids pYH207 (WT *flhDldr*-tR_2), pYH208 (ΔBS1 ΔBS2 *flhDldr*-tR_2), pYH209 (ΔE *flhDldr*-tR_2) and pYH210 (ΔBS1 ΔBS2 ΔE *flhDldr*-tR_2).

The amino-terminal hexahistidine-tagged RNase E expression vector p1VR122a was created by PCR amplification of the *rne* gene from *E. coli* strain MG1655. The resulting PCR product was digested with BamHI and PstI and cloned into the same sites of pCOLADuet-1 (Novagen).

Bacterial strains

E. coli strains used in this study are listed in Table 1. Details of the strain constructions are described in Supporting Information.

β-Galactosidase assays

Bacterial cultures were grown in LB supplemented with 100 μg/ml ampicillin at 30°C. Culture samples (4 ml) were harvested at various times during growth, washed with 10 mM Tris-HCl (pH 7.5) and frozen as cell pellets at −20°C. Cell extracts were prepared by suspending frozen cell pellets in 0.5 ml of BugBuster (Novagen). Following 30 min of incubation at 37°C, 0.3 ml of Z buffer containing 0.2 mg/ml lysozyme was added, incubation was then continued for 30 min at 37°C. After removal of cell debris, protein concentrations were determined by the Bio-Rad protein assay. β-galactosidase assays were performed using the cell extracts as described previously (Baker *et al.*, 2007).

RNA structure mapping and footprint assays

RNA was synthesized using the Ambion T7 MEGAscript kit and PCR-generated templates. Gel-purified RNA was dephosphorylated with calf intestinal alkaline phosphatase and then 5' end-labeled using T4 polynucleotide kinase (NEB) and [γ ^{32}P]ATP (7000 Ci/mmol). RNA suspended in Tris-EDTA buffer (TE) was renatured by heating to 85°C and cooling to room temperature. His-tagged *E. coli* CsrA (CsrA-H6) was purified as described (Mercante *et al.*, 2006). Binding reactions (10 μl) contained 10 mM Tris-HCl, pH 7.5, 10 mM $MgCl_2$, 100 mM KCl, 32.5 ng yeast RNA, 7.5% glycerol, 20 mM dithiothreitol (DTT), 4 U RNase inhibitor (Promega), 50 nM *flhDC* RNA, 200 μg/ml acetylated BSA, and various amounts of CsrA-H6. Reaction mixtures were incubated for 30 min at 37°C to allow CsrA–RNA complex formation. RNase T_1 (0.025 U) or RNase T_2 (0.03 U) was then added and incubation was continued for 15 min at 37°C. Reactions were terminated by adding 10 μl of stop buffer (95% formamide, 0.025% SDS, 20 mM EDTA, 0.025% bromophenol blue, 0.025% xylene cyanol, and 760 μg/ml yeast RNA) and placed on ice. Base hydrolysis and RNase T_1 digestion ladders were prepared as described (Bevilacqua and Bevilacqua, 1998). Samples were fractionated through 6% sequencing gels. Radioactive bands were visualized using a phosphorimager (Molecular Dynamics).

Gel mobility shift assay

Quantitative gel mobility shift assays of *flhDC* leader RNA followed a published procedure (Baker *et al.*, 2007). Binding reactions (10 μl) containing 0.1 nM 5' end-labeled *flhDC* leader RNA, various amounts of CsrA-H6, and 0.1 mg/ml xylene cyanol, were otherwise identical to the footprint assay. Competition assays also contained unlabeled RNA competitors. Following incubation at 37°C for 30 min, samples were fractionated on native 15% polyacrylamide gels. Free and bound RNA species were visualized with a phosphorimager and quantified using ImageQuant 5.2 software (Molecular Dynamics), and the apparent equilibrium binding constants (K_d) of CsrA–RNA interaction was calculated as described (Yakhnin and Babitzke, 2010). Mutant CsrA fusion protein encoded by the *csrA::kan* allele was purified as described for CsrA- H6 (Mercante *et al.*, 2006). Binding reactions contained 5' end-labeled 16-mer RNA containing a single high-affinity CsrA binding site (Dubey *et al.*, 2005; Mercante *et al.*, 2009) and either WT or mutant CsrA.

RNase E assay

Hexahistidine-tagged RNase E was purified by immobilized metal affinity chromatography using the following procedure. *E. coli* C43(DE3) (Lucigen) carrying p1VR122a was grown at 37° C in 1 L of Luria broth containing 50 μg/ml kanamycin to an OD_{600} of 0.7, at which time 1 mM isopropyl-β-D-thiogalactopyranoside (IPTG) was added and the culture was incubated for an additional 3 h at 37°C. Bacteria were harvested by centrifugation and suspended in 10 ml of buffer A (20 mM Tris-HCl, pH 7.9, 6 M guanidine-HCl, and 500 mM NaCl) containing 10 mM imidazole. Cells were lysed via sonication on ice, and unbroken cells were removed by centrifugation. Lysates were applied to a 1-ml HisTrap column (GE

Healthcare) previously equilibrated with buffer A containing 5 mM imidazole, washed with 10 ml buffer A containing 40 mM imidazole, and RNase E was eluted with a 30-ml linear imidazole gradient (30 to 500 mM) in buffer A. The elution peaks were established by SDS-PAGE. Purified, denatured RNase E was subjected to a series of refolding dialysis steps against buffer B (50 mM Tris-HCl, pH 7.9, 200 mM KCl, 10 mM $MgCl_2$, 1 mM DTT, and 20% [vol/vol] glycerol) containing 4 M guanidine-HCl, 2 M guanidine-HCl, and no denaturant. Insoluble protein was removed via ultracentrifugation for 15 min (100,000 x g) after each dialysis step. The resulting material was stored in buffer B containing 50% glycerol (vol/vol) at –20° C.

RNase E assays were performed *in vitro* by modifying published procedures (Perwez and Kushner, 2006). WT, ΔBS1 ΔBS2 or ΔE *flhDC* leader RNA (+1 to +210) was 5'end-labeled with γ [^{32}P]ATP and polynucleotide kinase. WT or ΔBS1 ΔBS2 *flhDC* leader RNA (+1 to +171) was 3'end-labeled using T4 RNA ligase (New England Biolabs) and [^{32}P]pCp (Perkin Elmer) using previously published reaction conditions (England and Uhlenbeck, 1978). RNAs were renatured in TE buffer by heating for 3 min at 85°C and cooling to room temperature. RNase E assays (45 μl) contained 25 or 40 nM RNA, 25 mM Tris-Cl, pH 7.9, 5 mM $MgCl_2$, 60 mM KCl, 100 mM NH_4Cl, 15 mM DTT, 7.5% glycerol, 1.5 mg/ml acetylated BSA, 4 U RNasin, RNase E (various amounts), ± 1 μM CsrA. Reaction mixtures were incubated for 30 min at 37°C to allow CsrA-RNA complex formation before adding RNase E. Incubation was continued at 37°C and 10 μl aliquots were removed at various times and quenched with 10 μl of footprint stop buffer, frozen in dry ice, and stored at −80°C. RNA samples were fractionated through 6% sequencing gels. Radioactive bands were visualized using a phosphorimager and quantified with ImageQuant 5.2.

Primer extension analysis to identify RNase E cleavage sites

Strains SK6632 (*rnb-500 pnp-200*) and SK6640 (*rnb-500 pnp-200 rne-1*) both containing plasmid pCSB81 (*flhDC* operon) were grown in LB with 100 μg/ml ampicillin at 30°C to late exponential phase. Cultures were then shifted to 44°C for 0, 1 or 5 min, at which time RNAprotect Bacteria reagent (Qiagen) was added to culture samples. Total RNA was isolated using the RNeasy Mini kit (Qiagen). The resulting RNA (15 μg) was annealed to 50 pmol of a 5' end-labeled oligo complementary to +256 to +277 of *flhDC* in TE buffer by heating to 70°C for 5 min and immediately placing on ice. Reverse transcription reactions (20 μl) were performed using the Verso cDNA synthesis kit (Thermo Scientific) according to the manufacturer's instructions. Reactions were incubated for 30 min at 42oC and stopped with an equal volume of loading buffer (95% formamide, 18 mM EDTA, 0.025% SDS, 0.025% xylene cyanol, and 0.025% bromophenol blue). Samples were fractionated through a taurine-buffered 6% sequencing gel. Sequencing reactions were performed using the same end-labeled primer and pCSB81 as template. Radioactive bands were visualized using a phosphorimager.

Quantitative analysis of flhDC transcript stability by primer extension

Strains containing chromosomally-integrated *flhD'-'lacZ* translational fusions or *flhD* leaders truncated at position +146 followed by the strong λ tR_2 intrinsic terminator (*flhD*-tR_2) were grown in 20 ml of LB in a shaking water bath at 30°C. Eight ml aliquots were harvested at late exponential phase growth and the remaining cultures were shifted to 44°C for 15 min, at which time additional 8 ml aliquots were harvested. Culture samples were mixed with 6 ml of frozen killing buffer (12 mM Tris-HCl, pH 7.2, 6 mM $MgCl_2$, 30 mM sodium azide, 15% ethanol, and 600 μg/ml chloramphenicol) and placed on ice. Following centrifugation, cell pellets were suspended in 1 ml of a 2:1 mixture of RNA Protect bacterial reagent (Qiagen):TE buffer, placed on ice for 10 min, and centrifuged. Cell pellets were frozen at −80 °C. Cells containing *flhD'-'lacZ* fusions were lysed and total RNA was

isolated using the RNeasy bacterial protocol (Qiagen). Cells containing truncated *flhD*-tR$_2$ leaders were lysed as above and the short transcripts were isolated using the miRNeasy kit (Qiagen). Oligonucleotide primers were 5′ end-labeled with [γ-^{32}P]ATP. A primer complementary to *lacZ* was used for the *flhD'-'lacZ* fusions, while a primer complementary to nt 69–91 of the *flhD* leader was used for the truncated *flhD*-tR$_2$ leader transcripts. In each case, primer extension of tmRNA using a primer complementary to nt 95–115 of mature tmRNA was used as a loading control. Two μg of RNA was annealed to 0.3 pmol of the labeled *lacZ* or *flhD* leader primer. As tmRNA is considerably more abundant than *flhD'-'lacZ* or *flhD*-tR$_2$ leader transcripts, a mixture of 0.15 pmol labeled and 3 pmol of unlabeled tmRNA primer was used to obtain primer extension signals that were similar in intensity to the *flhD'-'lacZ* or *flhD*-tR$_2$ leader signals. Annealing was performed in TE buffer by heating to 80°C for 3 min, followed by slow cooling to room temperature. Reverse transcription reactions (4 μl) contained the hybridization mixture and 1x Superscript III reverse transcriptase buffer, 0.5 mM dNTP, 0.8 U RNasin, 20 μg/ml acetylated BSA, 1 mM DTT, and 8 U of Superscript III reverse transcriptase (Invitrogen). Reactions were incubated for 30 min at 42°C and then quenched by adding 2.5 μl of stop buffer (20 mM EDTA, 95% formamide, 0.1% SDS, 0.05% xylene cyanol, and 0.05% bromphenol blue). Samples were heated for 5 min at 95°C prior to fractionating through standard 5% sequencing gels. Radioactive bands were visualized using a phosphorimager and quantified with ImageQuant 5.2.

mRNA half-life assay

Cultures were grown at 30°C in tryptone broth supplemented with ampicillin (100 μg/ml) to late exponential phase prior to the addition of rifampicin (200 μg/ml) to prevent transcription initiation. After 1 min, 10 ml aliquots were removed at various times and added to an equal volume of frozen buffer (10 mM Tris-HCl, pH 7.2, 5 mM $MgCl_2$, 25 mM sodium azide, 12.5% ethanol, and 500 μg/ml choramphenicol). Cells were collected by centrifugation and cell pellets were suspended in 1 ml of a 2:1 mixture of RNAProtect bacterial reagent:TE buffer and placed on ice for 10 min. Cells were then collected by centrifugation and cell pellets were frozen at −80°C. RNA was isolated using the RNeasy Mini kit. DNA was removed with 1 U of Turbo DNase (Ambion). The RNA was extracted with phenol, precipitated and suspended in water. Quantification by Northern blot analysis followed a published procedure (Oh *et al.*, 2009). Ten micrograms of total RNA was mixed with at least two volumes of denaturing solution (66% formamide, 9% formaldehyde, 20 mM MOPS, pH 7.0, 5 mM NaOAc, and 2 mM EDTA) and then heated for 15 min at 65°C. RNA samples (8 μg) were separated by electrophoresis through a 1.2% denaturing formaldehyde agarose gel. RNA was transferred to Hybond N+ membranes (Amersham) by capillary blotting with 10x SSC (1.5 M NaCl and 150 mM sodium citrate, pH 7.0) and fixed to the membrane by heating at 80°C for 2 h under vacuum. Fixed membranes were prehybridized at 46°C for 3 hr in hybridization buffer (7% SDS, 0.5 M sodium phosphate, pH 7.2, 10 mM EDTA, and 0.0125% nonfat powdered milk). Hybridization was with a 5' end-labeled probe complementary to the *flhDC* leader ($2x10^6$ cpm/mL final concentration) in hybridization buffer for 15 hr at 46°C. Membranes were washed three times for 20 min each with Buffer 1 (2x SSC and 0.1% SDS) at 37°C, followed by three 20-min washes with Buffer 2 (1x SSC and 0.1% SDS) at 42°C. mRNA levels were quantified with a phosphorimager and ImageQuant 5.2 software. Before reprobing, membranes were stripped by boiling in 0.2% SDS for 5 min and then hybridized with a 16S rRNA oligonucleotide probe at 52°C as described above. Each *flhDC* data point was normalized to the 16S rRNA value before calculating mRNA the half-live as described (Yakhnin *et al.*, 2001).

Supplementary Material

Refer to Web version on PubMed Central for supplementary material.

Acknowledgments

We thank Sidney Kushner for bacterial strains. This work was supported by NIH grant GM059969 and CRIS project FLA-MCS-004949.

References

Arraiano CM, Andrade JM, Domingues S, Guinote IB, Malecki M, Matos RG, et al. The critical role of RNA processing and degradation in the control of gene expression. FEMS Microbiol Rev. 2010; 34:883–923. [PubMed: 20659169]

Arraiano CM, Yancey SD, Kushner SR. Stabilization of discrete mRNA breakdown products in *ams pnp rnb* multiple mutants of *Escherichia coli* K-12. J Bacteriol. 1988; 170:4625–4633. [PubMed: 2459106]

Babitzke P, Kushner SR. The Ams (altered mRNA stability) protein and ribonuclease E are encoded by the same structural gene of *Escherichia coli*. Proc Natl Acad Sci USA. 1991; 88:1–5. [PubMed: 1846032]

Babitzke P, Romeo T. CsrB sRNA family: sequestration of RNA-binding regulatory proteins. Curr Opin Microbiol. 2007; 10:156–163. [PubMed: 17383221]

Baker CS, Eöry LA, Yakhnin H, Mercante J, Romeo T, Babitzke P. CsrA inhibits translation initiation of *Escherichia coli hfq* by binding to a single site overlapping the Shine-Dalgarno sequence. J Bacteriol. 2007; 189:5472–5481. [PubMed: 17526692]

Bevilacqua JM, Bevilacqua PC. Thermodynamic analysis of an RNA combinatorial library contained in a short hairpin. Biochemistry. 1998; 37:15877–15884. [PubMed: 9843393]

Bolivar F, Rodriguez RL, Greene PJ, Betlach MC, Heyneker HL, Boyer HW, et al. Construction and characterization of new cloning vehicles. II. A multipurpose cloning system. Gene. 1977; 2:95–113. [PubMed: 344137]

Callaghan AJ, Marcaida MJ, Stead JA, McDowall KJ, Scott WG, Luisi BF. Structure of *Escherichia coli* RNase E catalytic domain and implications for RNA turnover. Nature. 2005; 437:1187–1191. [PubMed: 16237448]

Carpousis AJ. The RNA degradosome of *Escherichia coli*: an mRNA-degrading machine assembled on RNase E. Annu Rev Microbiol. 2007; 61:71–87. [PubMed: 17447862]

Chavez RG, Alvarez AF, Romeo T, Georgellis D. The physiological stimulus for the BarA sensor kinase. J Bacteriol. 2010; 192:2009–2012. [PubMed: 20118252]

Deana A, Celesnik H, Belasco JG. The bacterial enzyme RppH triggers messenger RNA degradation by 5' pyrophosphate removal. Nature. 2008; 451:355–358. [PubMed: 18202662]

Dubey AK, Baker CS, Suzuki K, Jones AD, Pandit P, Romeo T, Babitzke P. CsrA regulates translation of the *Escherichia coli* carbon starvation gene, *cstA*, by blocking ribosome access to the *cstA* transcript. J Bacteriol. 2003; 185:4450–4460. [PubMed: 12867454]

Dubey AK, Baker CS, Romeo T, Babitzke P. RNA sequence and secondary structure participate in high-affinity CsrA-RNA interaction. RNA. 2005; 11:1579–1587. [PubMed: 16131593]

Edwards AN, Patterson-Fortin LM, Vakulskas CA, Mercante JW, Potrykus K, Camacho MI, et al. Circuitry linking the Csr and stringent response global regulatory systems. Mol Microbiol. 2011; 80:1561–1580. [PubMed: 21488981]

England TE, Uhlenbeck OC. 3'-terminal labelling of RNA with T4 RNA ligase. Nature. 1978; 275:560–561. [PubMed: 692735]

Gao J, Lee K, Zhao M, Qiu J, Zhan X, Saxena A, et al. Differential modulation of *E. coli* mRNA abundance by inhibitory proteins that alter the composition of the degradosome. Mol Microbiol. 2006; 61:394–406. [PubMed: 16771842]

Haldimann A, Wanner BL. Conditional-replication, integration, excision, and retrieval plasmid-host systems for gene structure-function studies of bacteria. J Bacteriol. 2001; 183:6384–6393. [PubMed: 11591683]

Kime L, Jourdan SS, McDowall KJ. Identifying and characterizing substrates of the RNase E/G family of enzymes. Methods Enzymol. 2008; 447:215–241. [PubMed: 19161846]

Kime L, Jourdan SS, Stead JA, Hidalgo-Sastre A, McDowall KJ. Rapid cleavage of RNA by RNase E in the absence of 5' monophosphate stimulation. Mol Microbiol. 2010; 76:590–604. [PubMed: 19889093]

Lehnen D, Blumer C, Polen T, Wackwitz B, Wendisch VF, Unden G. LrhA as a new transcriptional key regulator of flagella, motility and chemotaxis genes in *Escherichia coli*. Mol Microbiol. 2002; 45:521–532. [PubMed: 12123461]

Liu MY, Gui G, Wei B, Preston JF III, Oakford L, Yuksel U, et al. The RNA molecule CsrB binds to the global regulatory protein CsrA and antagonizes its activity in *Escherichia coli*. J Biol Chem. 1997; 272:17502–17510. [PubMed: 9211896]

Liu MY, Romeo T. The global regulator CsrA of *Escherichia coli* is a specific mRNA-binding protein. J Bacteriol. 1997; 179:4639–4642. [PubMed: 9226279]

McDowall KJ, Lin-Chao S, Cohen SN. A+U content rather than a particular nucleotide order determines the specificity of RNase E cleavage. J Biol Chem. 1994; 269:10790–10796. [PubMed: 7511606]

Mackie GA. Ribonuclease E is a 5'-end-dependent endonuclease. Nature. 1998; 395:720–723. [PubMed: 9790196]

Mercante J, Suzuki K, Cheng X, Babitzke P, Romeo T. Comprehensive alanine-scanning mutagenesis of *Escherichia coli* CsrA defines two subdomains of critical functional importance. J Biol Chem. 2006; 281:31832–31842. [PubMed: 16923806]

Mercante J, Edwards AN, Dubey AK, Babitzke P, Romeo T. Molecular geometry of CsrA (RsmA) binding to RNA and its implications for regulated expression. J Mol Biol. 2009; 392:511–528. [PubMed: 19619561]

Mohanty BK, Kushner SR. Processing of the *Escherichia coli leuX* tRNA transcript, encoding $tRNA^{Leu5}$, requires either the 3' to 5' exoribonuclease polynucleotide phosphorylase or RNase P to remove the Rho-independent transcription terminator. Nucleic Acids Res. 2010; 38:597–607. [PubMed: 19906695]

Oh HS, Pathak HB, Goodfellow IG, Arnold JJ, Cameron CE. Insight into poliovirus genome replication and encapsidation obtained from studies of 3B-3C cleavage site mutants. J Virol. 2009; 83:9370–9387. [PubMed: 19587035]

Ow MC, Liu Q, Kushner SR. Analysis of mRNA decay and rRNA processing in *Escherichia coli* in the absence of RNase E-based degradosome assembly. Mol Microbiol. 2000; 38:854–866. [PubMed: 11115119]

Pannuri A, Yakhnin H, Vakulskas CA, Edwards AN, Babitzke P, Romeo T. Translational repression of NhaR, a novel pathway for multi-tier regulation of biofilm circuitry by CsrA. J Bacteriol. 2012; 194:79–89. [PubMed: 22037401]

Perwez T, Kushner SR. RNase Z in *Escherichia coli* plays a significant role in mRNA decay. Mol Microbiol. 2006; 60:723–737. [PubMed: 16629673]

Prüß BM, Matsumura P. Cell cycle regulation of flagellar genes. J Bacteriol. 1997; 179:5602–5604. [PubMed: 9287021]

Richards J, Luciano DJ, Belasco JG. Influence of translation on RppH-dependent mRNA degradation in *Escherichia coli*. Mol Microbiol. 2012 [Epub ahead of print]. 10.1111/mmi.12040

Romeo T, Gong M, Liu MY, Brun-Zinkernagel AM. Identification and molecular characterization of *csrA*, a pleiotropic gene from *Escherichia coli* that affects glycogen biosynthesis, gluconeogenesis, cell size, and surface properties. J Bacteriol. 1993; 175:4744–4755. [PubMed: 8393005]

Romeo T, Vakulskas CA, Babitzke P. Posttranscriptional regulation on a global scale: Form and function of Csr/Rsm systems. Env Microbiol. 2012 (Epub ahead of print). 10.1111/j.1462-2920.2012.02794.x

Sabnis NA, Yang H, Romeo T. Pleiotropic regulation of central carbohydrate metabolism in *Escherichia coli* via the gene *csrA*. J Biol Chem. 1995; 270:29096–29104. [PubMed: 7493933]

Schubert M, Lapouge K, Duss O, Oberstrass FC, Jelesarov I, Haas D, Allain FH. Molecular basis of messenger RNA recognition by the specific bacterial repressing clamp RsmA/CsrA. Nat Struct Mol Biol. 2007; 14:807–813. [PubMed: 17704818]

Shin S, Park C. Modulation of flagellar expression in *Escherichia coli* by acetyl phosphate and the osmoregulator OmpR. J Bacteriol. 1995; 177:4696–4702. [PubMed: 7642497]

Smith TG, Hoover TR. Deciphering bacterial flagellar gene regulatory networks in the genomic era. Adv Appl Microbiol. 2009; 67:257–295. [PubMed: 19245942]

Soutourina O, Kolb A, Krin E, Laurent-Winter C, Rimsky S, Danchin A, Bertin P. Multiple control of flagellum biosynthesis in *Escherichia coli*: role of H-NS protein and the cyclic AMP-catabolite activator protein complex in transcription of the *flhDC* master operon. J Bacteriol. 1999; 181:7500–7508. [PubMed: 10601207]

Sperandio V, Torres AG, Kaper JB. Quorum sensing *Escherichia coli* regulators B and C (QseBC): a novel two-component regulatory system involved in the regulation of flagella and motility by quorum sensing in *E. coli*. Mol Microbiol. 2002; 43:809–821. [PubMed: 11929534]

Stead MB, Marshburn S, Mohanty BK, Mitra J, Castillo LP, Ray D, et al. Analysis of *Escherichia coli* RNase E and RNase III activity *in vivo* using tiling microarrays. Nucleic Acids Res. 2011; 39:3188–3203. [PubMed: 21149258]

Suzuki K, Wang X, Weilbacher T, Pernestig AK, Melefors Ö, Georgellis D, et al. Regulatory circuitry of the CsrA/CsrB and BarA/UvrY systems of *Escherichia coli*. J Bacteriol. 2002; 184:5130–5140. [PubMed: 12193630]

Suzuki K, Babitzke P, Kushner SR, Romeo T. Identification of a novel regulatory protein (CsrD) that targets the global regulatory RNAs CsrB and CsrC for degradation by RNase E. Genes Dev. 2006; 20:2605–2617. [PubMed: 16980588]

Thomason MK, Fontaine F, De Lay N, Storz G. A small RNA that regulates motility and biofilm formation in response to changes in nutrient availability in *Escherichia coli*. Mol Microbiol. 2012; 84:17–35. [PubMed: 22289118]

Timmermans J, Van Melderen L. Conditional essentiality of the *csrA* gene in *E. coli*. J Bacteriol. 2009; 191:1722–1724. [PubMed: 19103924]

Wang S, Fleming RT, Westbrook EM, Matsumura P, McKay DB. Structure of the *Escherichia coli* FlhDC complex, a prokaryotic heteromeric regulator of transcription. J Mol Biol. 2006; 355:798–808. [PubMed: 16337229]

Wei BL, Brun-Zinkernagel AM, Simecka JW, Prüß BM, Babitzke P, Romeo T. Positive regulation of motility and *flhDC* expression by the RNA-binding protein CsrA of *Escherichia coli*. Mol Microbiol. 2001; 40:245–256. [PubMed: 11298291]

Weilbacher T, Suzuki K, Dubey AK, Wang X, Gudapaty S, Morozov I, et al. A novel sRNA component of the carbon storage regulatory system of *Escherichia coli*. Mol Microbiol. 2003; 48:657–670. [PubMed: 12694612]

Yakhnin AV, Babitzke P. Mechanism of NusG-stimulated pausing, hairpin-dependent pause site selection and intrinsic termination at overlapping pause and termination sites in the *Bacillus subtilis trp* leader. Mol Microbiol. 2010; 76:690–705. [PubMed: 20384694]

Yakhnin H, Babiarz JE, Yakhnin AV, Babitzke P. Expression of the *Bacillus subtilis trpEDCFBA* operon is influenced by translational coupling and Rho termination factor. J Bacteriol. 2001; 183:5918–5926. [PubMed: 11566991]

Yakhnin H, Yakhnin AV, Baker CS, Sineva E, Berezin I, Romeo T, Babitzke P. Complex regulation of the global regulatory gene *csrA*: CsrA-mediated translational repression, transcription from five promoters by $E\sigma^{70}$ and $E\sigma^{S}$, and indirect transcriptional activation by CsrA. Mol Microbiol. 2011a; 81:689–704. [PubMed: 21696456]

Yakhnin H, Baker CS, Berezin I, Evangelista MA, Rassin A, Romeo T, Babitzke P. CsrA represses translation of *sdiA*, which encodes the N-acylhomoserine-L-lactone receptor of *Escherichia coli*, by binding exclusively within the coding region of *sdiA* mRNA. J Bacteriol. 2011b; 193:6162–6170. [PubMed: 21908661]

Yancey SD, Kushner SR. Isolation and characterization of a new temperature-sensitive polynucleotide phosphorylase mutation in *Escherichia coli* K-12. Biochimie. 1990; 72:835–843. [PubMed: 2085546]

Zuker M. Mfold web server for nucleic acid folding and hybridization prediction. Nucleic Acids Res. 2003; 31:3406–3415. [PubMed: 12824337]

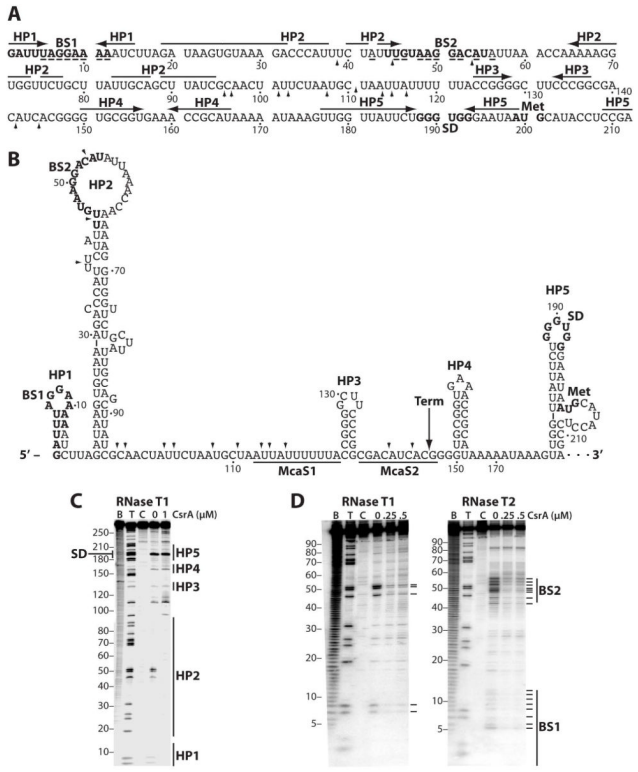

Fig. 1. *flhDC* leader RNA and CsrA-*flhDC* leader RNA footprint analysis

A. Sequence of *flhDC* leader RNA. The CsrA binding sites (BS1 and BS2), the *flhD* Shine-Dalgarno (SD) sequence and translation initiation codon (Met) are in bold. Hairpins 1–5 (HP1-HP5) are shown with horizontal arrows. Residues protected by CsrA from RNase T_1 or RNase T_2 cleavage are indicated with a (–) below the residue. Arrowheads mark RNase E cleavage sites identified *in vitro*. Numbering is with respect to the start of transcription.

B. Secondary structure of *flhDC* leader RNA. Hairpins 1–5 (HP1-HP5) are shown. Positions of the CsrA binding sites (BS1 and BS2), the *flhD* Shine-Dalgarno (SD) sequence and translation initiation codon (Met) are in bold. Arrowheads mark RNase E cleavage sites identified *in vitro*. Binding sites for McaS sRNA (McaS1 and McaS2) are underlined. A long vertical arrow indicates the position of an engineered λtR_2 terminator (Term). Numbering is with respect to the start of transcription.

C. RNA structure mapping of an *flhDC* transcript extending from +1 to +276. 5’ end-labeled RNA was treated with RNase T_1. Experimental samples contained 0 or 1 μM CsrA. Partial alkaline hydrolysis (B) and RNase T_1 digestion (T) ladders, and control lanes without Rnase treatment (C), are shown. The RNase T_1 ladder was generated under denaturing conditions (3 M urea at 55°C) so that every G residue could be observed. Positions of the *flhD* Shine-Dalgarno (SD) sequence and HP1-HP5 are shown.

D. CsrA-*flhDC* RNA footprint analysis. 5’ end-labeled RNA (+1 to +99) was treated with RNase T_1 or RNase T_2 in the absence or presence of 0.25 or 0.5 μM CsrA. Partial alkaline hydrolysis (B) and RNase T_1 digestion (T) ladders, and control lanes without RNase treatment (C), are shown. Residues in which bound CsrA reduced RNase cleavage are marked on the right of each gel (–). Positions of the CsrA binding sites (BS1 and BS2) are shown.

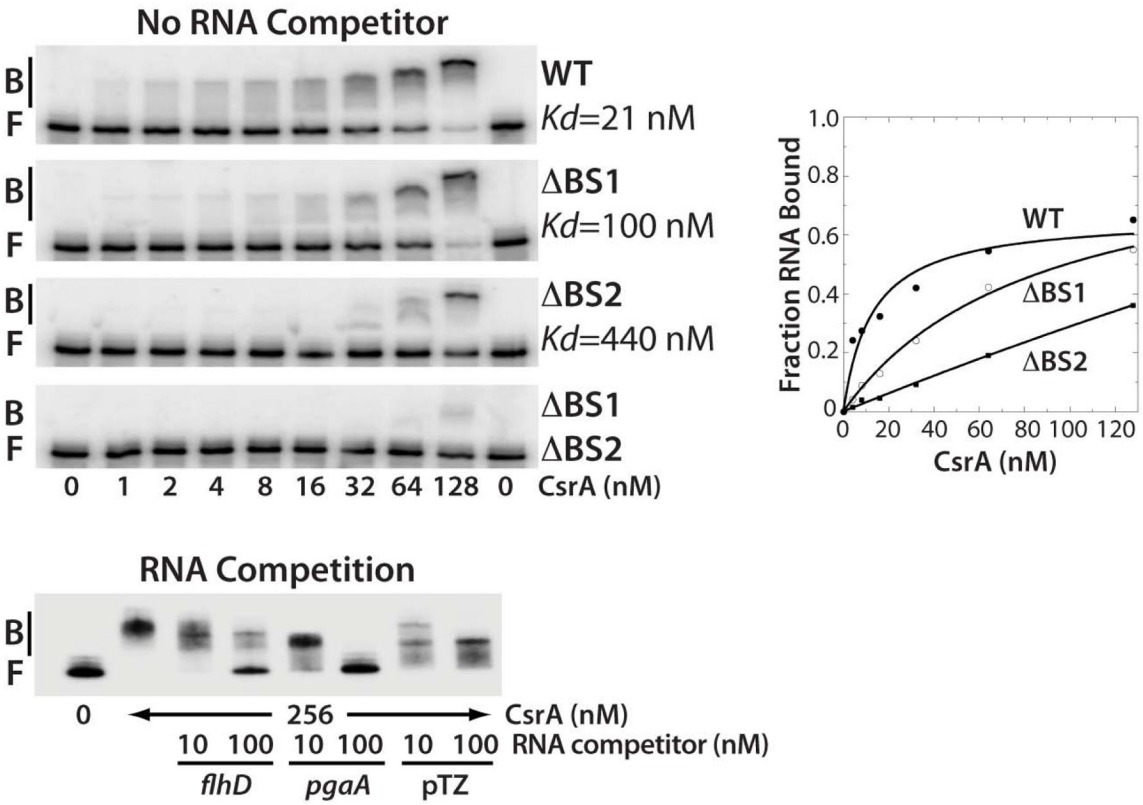

Fig. 2. Gel mobility shift analysis of CsrA-*flhDC* leader RNA interaction

5' end-labeled RNA was incubated with the concentration of CsrA indicated at the bottom of each lane. Positions of bound (B) and free (F) *flhDC* leader RNA are marked. K_d values of CsrA interaction with wild type (WT), ΔBS1, ΔBS2 and ΔBS1 ΔBS2 mutant transcripts are shown. The simple binding curve for these data is shown at the right. For the RNA competition assay, labeled *flhDC* leader RNA was incubated with CsrA ± 10- or 100-fold excess of specific (*flhD* and *pgaA*) or non-specific (pTZ19R) competitor RNA.

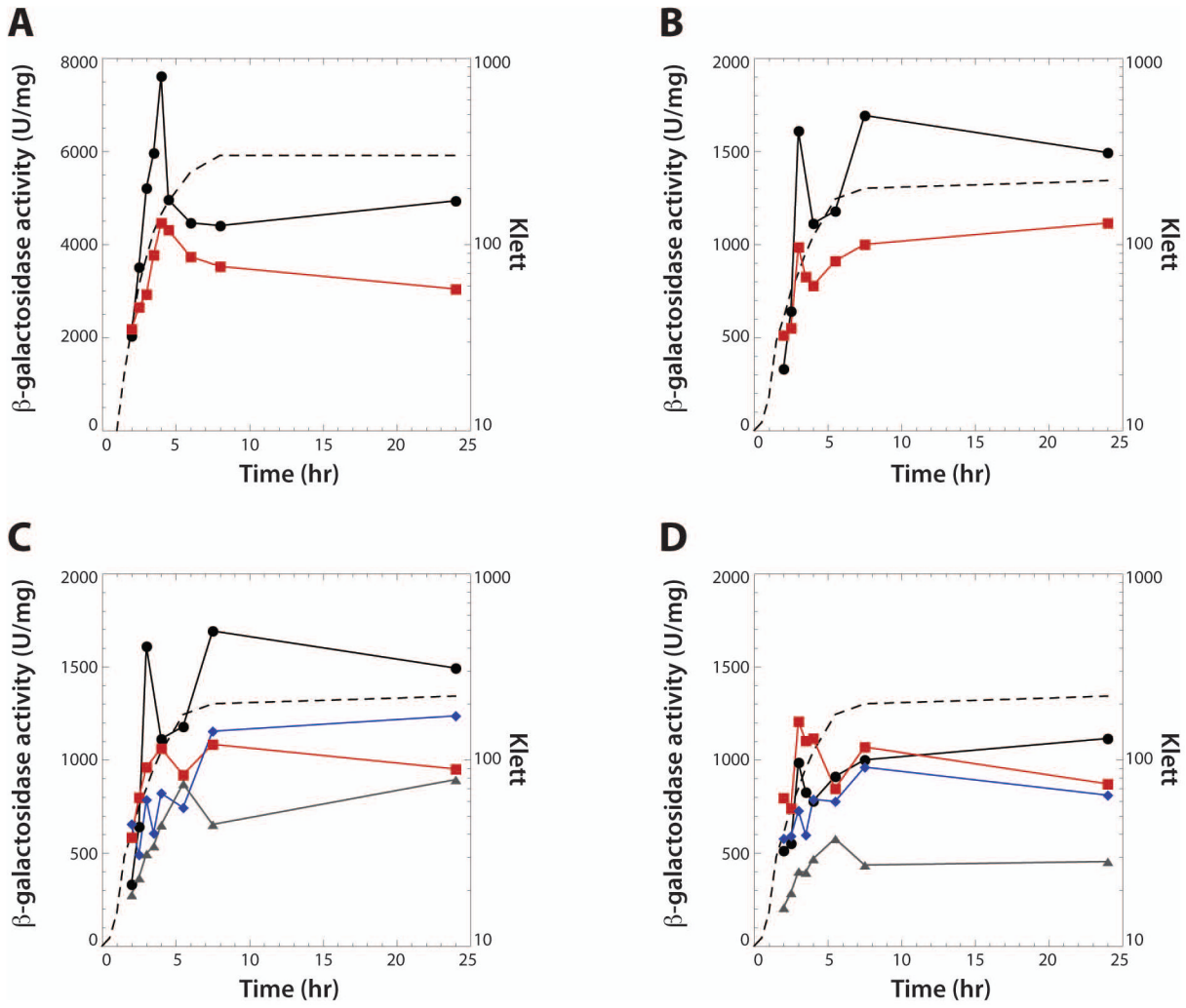

Fig. 3. CsrA-dependent regulation of *flhDC* expression

Cells were grown in LB at 30°C. Representative growth curves are shown with a dashed line in each panel.γ-galactosidase values are averages of at least two independent experiments.

A. Effect of *csrA* on expression of a plasmid-borne *flhDC'-'lacZ* translational fusion. Symbols are: WT, black circles; *csrA*, red squares.

B. Effect of *csrA* on expression of a chromosomally integrated *flhD'-'lacZ* translational fusion. Symbols are: WT, black circles; *csrA*, red squares.

C. Effect of CsrA binding sites on expression of chromosomally integrated *flhD'-'lacZ* translational fusions in WT (*csrA+*) strains. Symbols are: WT, black circles; ΔBS1, red squares;ΔBS2, blue diamonds; ΔBS1 ΔBS2, grey triangles.

D. Effect of CsrA binding sites on expression of chromosomally integrated *flhD'-'lacZ* translational fusions in *csrA* mutant strains. Symbols are: WT, black circles; ΔBS1, red squares;ΔBS2, blue diamonds; ΔBS1 ΔBS2, grey triangles.

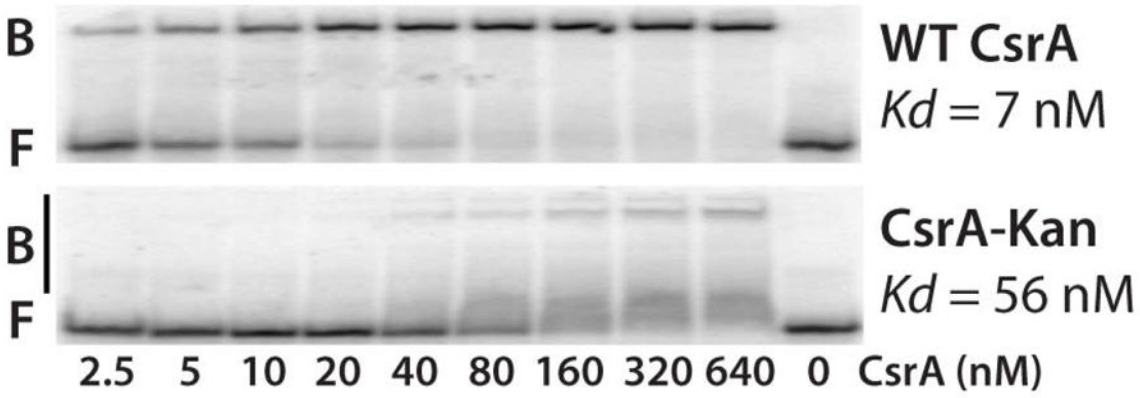

Fig. 4. Gel mobility shift analysis of WT and mutant CsrA protein

5’ end-labeled RNA was incubated with the concentration of WT or mutant CsrA shown at the bottom of each lane. Positions of bound (B) and free (F) RNA are shown.

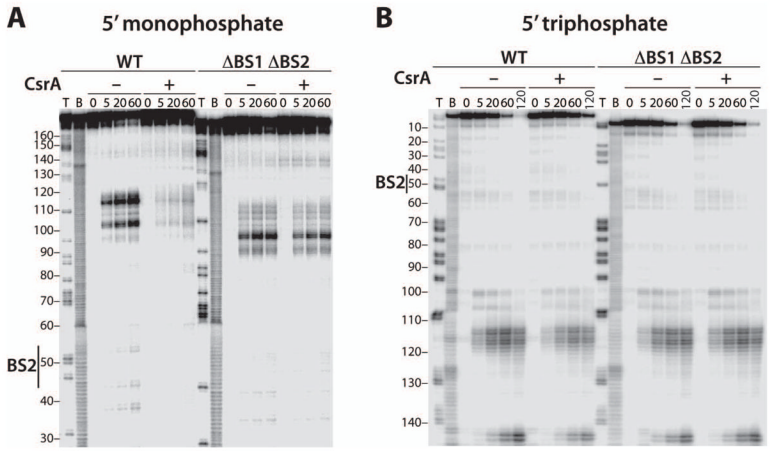

Fig. 5. RNase E cleavage of WT and ΔBS1 ΔBS2 *flhDC* leader RNA

A. 5’ end-labeled WT or ΔBS1 ΔBS2 RNAs containing 5' monophosphate ends were treated with 8 nM RNase E for the indicated times in the absence (–) or presence (+) of 1 μM CsrA. Partial alkaline hydrolysis (B) and RNase T_1 digestion (T) ladders are shown. Position of CsrA binding site 2 (BS2) is marked. Numbering is with respect to the start of transcription.

B. 3' end-labeled WT or ΔBS1 ΔBS2 RNAs containing 5' triphosphate ends were treated with 25 nM RNase E for the indicated times in the absence (–) or presence (+) of 1 μM CsrA. Partial alkaline hydrolysis (B) and RNase T_1 digestion (T) ladders are shown. Position of CsrA binding site 2 (BS2) is marked. Numbering is with respect to the start of transcription.

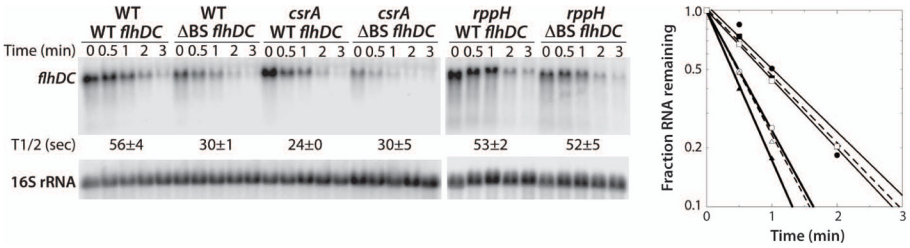

Fig. 6. Northern blot analysis of *flhDC* mRNA half-life

mRNA half-life experiments of wild type (WT) or ΔBS1 ΔBS2 mutant (ΔBS) *flhDC* mRNA were performed in wild type (WT), *csrA* or *rppH* strains. Cultures were grown at 30°C to late exponential phase prior to the addition of rifampicin. After 1 min, samples were harvested at the indicated times. mRNA half-lives ($T_{1/2}$) are shown. 16S rRNA blots are shown as loading controls. The level of *flhDC* mRNA was normalized to the 16S rRNA level in each lane. Quantification of these data is shown at the right. Symbols are: WT *flhDC*, solid circles; ΔBS1 ΔBS2 *flhDC*, open circles; WT *flhDC csrA*, solid triangles; ΔBS1 ΔBS2 *flhDC csrA*, open triangles (dashed line); WT *flhDC rppH*, solid squares (dashed line); ΔBS1 ΔBS2 *flhDC rppH*, open squares.

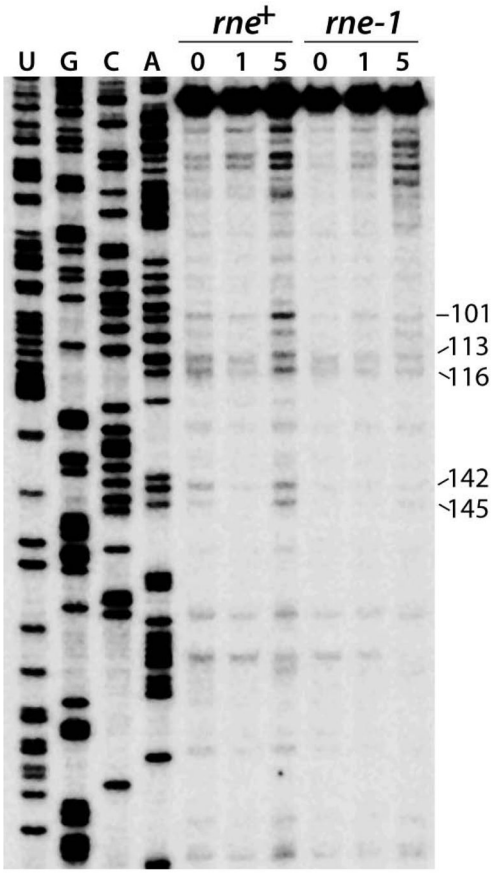

Fig. 7. Primer extension analysis of RNase E cleavage sites in *flhDC* leader RNA

RNA was isolated from *pnp rnb* and *pnp rnb rne* mutant strains containing pCSB81 (*flhDC*) at 0, 1 or 5 min after a shift to the non-permissive temperature (44°C). A primer specific for *lacZ* was annealed to total cellular RNA and extended by reverse transcriptase. Positions of *flhDC* leader RNA 5' ends are marked on the right. DNA sequencing ladder is shown.

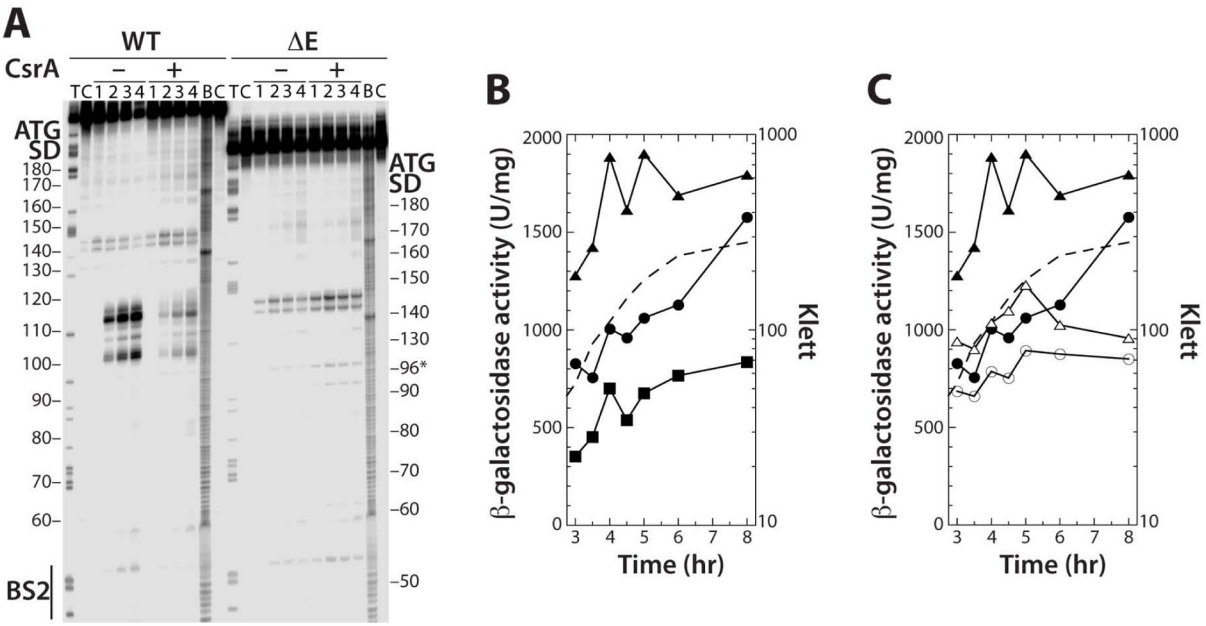

Fig. 8. Effects of deleting RNase E cleavage sites on *flhDC* expression

A. 5' end-labeled WT orΔE RNAs were treated with 4 nM RNase E for 0 (lane 1), 5 (lane 2), 20 (lane 3) or 60 (lane 4) min in the absence (–) or presence (+) of 1 μM CsrA. Partial alkaline hydrolysis (B) and RNase T_1 digestion (T) ladders, and control lanes without RNase treatment

(C), are shown. Positions of CsrA binding site 2 (BS2), as well as the *flhD* Shine-Dalgarno (SD) sequence and start codon are marked.

B. WT, ΔBS1 ΔBS2 and ΔE chromosomally integrated *flhD'-'lacZ* translational fusions in WT backgrounds were grown in LB at 30°C. Each experiment was performed at least twice and γ-galactosidase values from a representative experiment are shown. Symbols are: WT fusion, solid circles; ΔE fusion, solid triangles; ΔBS1 ΔBS2, solid squares. A representative growth curve is shown with a dashed line.

C. WT and ΔE chromosomally integrated *flhD'-'lacZ* translational fusions in WT and *csrA* mutant backgrounds were grown in LB at 30°C. Each experiment was performed at least three times and γ-galactosidase values from a representative experiment are shown. Symbols are: WT fusion, solid circles; WT fusion *csrA*, open circles; ΔE fusion, solid triangles; ΔE fusion *csrA*, open triangles. A representative growth curve is shown with a dashed line.

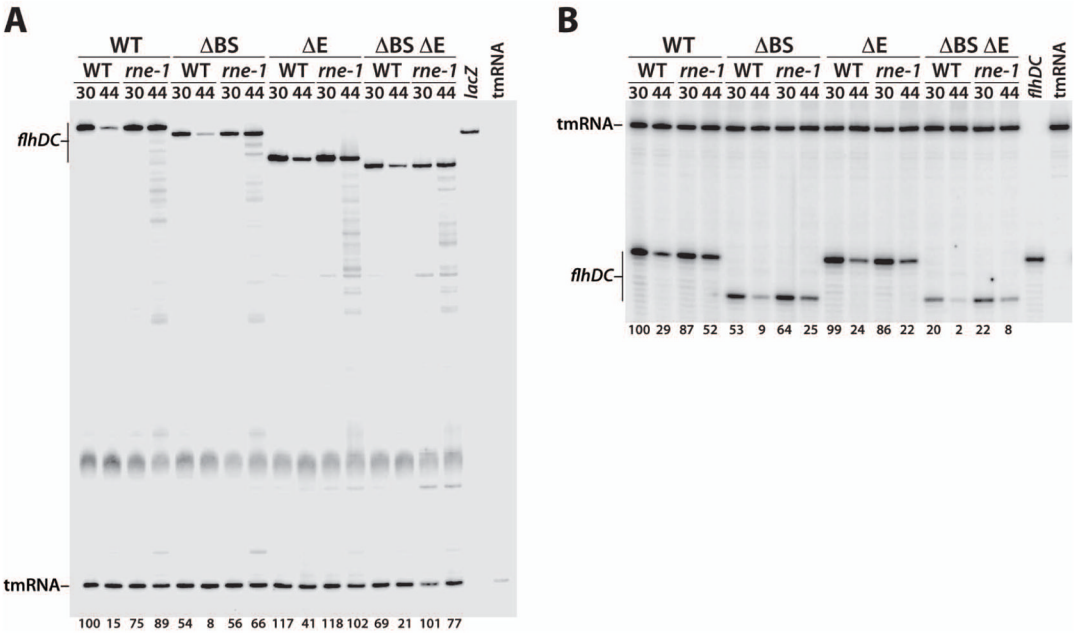

Fig. 9. Quantitative primer extension analysis of WT, ΔBS, ΔE and ΔBS ΔE transcript decay

RNA was isolated from WT and *rne* mutant strains containing chromosomally integrated *flhD'-'lacZ* fusions (A) or truncated *flhD*-tR_2 constructs (B). Cells were grown at 30°C and harvested before or after a shift to the non-permissive temperature (44°C).

A. Primers specific for *lacZ* mRNA and tmRNA were annealed simultaneously to total cellular RNA and extended by reverse transcriptase. Levels of full-length *flhDC* transcripts were normalized to tmRNA levels. The level of RNA for the WT transcript in the WT (*rne+*) genetic background at 30°C was set to 100%. Normalized RNA levels are shown at the bottom of each lane. Control reactions with only the *lacZ* or tmRNA primers are marked.

B. Primers specific for *flhDC* leader and tmRNA were annealed simultaneously to total cellular RNA and extended by reverse transcriptase. Levels of full-length *flhDC* transcripts were normalized to tmRNA levels. The level of RNA for the WT transcript in the WT (*rne+*) genetic background at 30°C was set to 100%. Normalized RNA levels are shown at the bottom of each lane. Control reactions with only the *flhDC* leader or tmRNA primers are marked. Since the *flhDC* leader primer hybridizes upstream of the ΔE deletion, the length of the primer extension products for WT and ΔE, as well as for ΔBS and ΔBS ΔE, are the same.

Table 1

E. coli strains used in this study

Strain	Description[a]	Source
C43(DE3)	F⁻ *ompT hsdSB (rB- mB-) gal dcm* (DE3)	Lucigen
CF7789	F⁻ λ⁻Δ*lacI-lacZ* (*Mlu*I)	Wei *et al*, 2001
MG1655	Prototrophic F- λ-	M. Cashel
PLB441	MG1655/*flhDldr::kan*	This study
PLB442	CF7789 *uvrY::cam flhDldr::kan*	This study
PLB931	CF7789/pFDCZ6 (*flhDC'-'lacZ*) Ap^r	This study
PLB932	CF7789/*csrA::kan* pFDCZ6 (*flhDC'-'lacZ*) Ap^r	This study
PLB966	CF7789/*uvrY::cam csrA::kan*	This study
PLB1258	CF7789/*flhD'-'lacZ* Ap^r	This study
PLB1259	CF7789/ΔBS1 *flhD'-'lacZ* Ap^r	This study
PLB1260	CF7789/ΔBS2 *flhD'-'lacZ* Ap^r	This study
PLB1262	CF7789/ΔBS1 ΔBS2 *flhD'-'lacZ* Ap^r	This study
PLB1263	CF7789/*csrA::kan flhD'-'lacZ* Ap^r	This study
PLB1264	CF7789/*csrA::kan* ΔBS1 *flhD'-'lacZ* Ap^r	This study
PLB1265	CF7789/*csrA::kan* ΔBS2 *flhD'-'lacZ* Ap^r	This study
PLB1266	CF7789/*csrA::kan* ΔBS1 ΔBS2 *flhD'-'lacZ* Ap^r	This study
PLB1601	CF7789/*uvrY::cam rppH::kan*	This study
PLB1618	CF7789/*uvrY::cam csrA::kan* pCSB81 Ap^r	This study
PLB1619	CF7789/*uvrY::cam rppH::kan* pCSB81 Ap^r	This study
PLB1620	CF7789/*uvrY::cam* pCSB81 Ap^r	This study
PLB1625	CF7789/*uvrY::cam* pCSB83 Ap^r	This study
PLB1626	CF7789/*uvrY::cam rppH::kan* pCSB83 Ap^r	This study
PLB1627	CF7789/*uvrY::cam csrA::kan* pCSB83 Ap^r	This study
PLB1646	SK6632/pCSB81 (*flhDC*) Ap^r	This study
PLB1647	SK6640/pCSB81 (*flhDC*) Ap^r	This study
PLB1759	CF7789/ΔE *flhD'-'lacZ* Ap^r	This study
PLB1760	CF7789/*csrA::kan* ΔE *flhD'-'lacZ* Ap^r	This study
PLB1762	CF7789/*rppH::kan*	This study
PLB1768	CF7789/*uvrY::cam flhD'-'lacZ* Ap^r	This study
PLB1770	CF7789/*uvrY::cam* ΔBS1 ΔBS2 *flhD'-'lacZ* Ap^r	This study
PLB1771	CF7789/*uvrY::cam* ΔE *flhD'-'lacZ* Ap^r	This study
PLB1773	CF7789/*uvrY::cam rppH::kan flhD'-'lacZ* Ap^r	This study
PLB1774	CF7789/*uvrY::cam rppH::kan* ΔBS1 ΔBS2 *flhD'-'lacZ* Ap^r	This study
PLB1775	CF7789/*uvrY::cam rppH::kan* ΔE *flhD'-'lacZ* Ap^r	This study
PLB1776	CF7789/*rppH::kan flhD'-'lacZ* Ap^r	This study
PLB1777	CF7789/*rppH::kan* ΔBS1 ΔBS2 *flhD'-'lacZ* Ap^r	This study
PLB1778	CF7789/*rppH::kan* ΔE *flhD'-'lacZ* Ap^r	This study

PLB1812	CF7789/*uvrY::cam pyrC::Tn*10 *flhD'-'lacZ* Ap^r	This study
PLB1813	CF7789/*uvrY::cam pyrC::Tn*10 ΔBS1 ΔBS2 *flhD'-'lacZ* Ap^r	This study
PLB1814	CF7789/*uvrY::cam pyrC::Tn*10 ΔE *flhD'-'lacZ* Ap^r	This study
PLB1816	CF7789/*uvrY::cam rne-1 flhD'-'lacZ* Ap^r	This study
PLB1817	CF7789/*uvrY::cam rne-1* ΔBS1 ΔBS2 *flhD'-'lacZ* Ap^r	This study
PLB1818	CF7789/*uvrY::cam rne-1* ΔE *flhD'-'lacZ* Ap^r	This study
PLB1832	CF7789/*uvrY::cam* ΔBS1 ΔBS2 ΔE *flhD'-'lacZ* Ap^r	This study
PLB1845	CF7789/*uvrY::cam pyrC::Tn*10 ΔBS1 ΔBS2 ΔE *flhD'-'lacZ* Ap^r	This study
PLB1846	CF7789/*uvrY::cam rne-1* ΔBS1 ΔBS2 ΔE *flhD'-'lacZ* Ap^r	This study
PLB1852	CF7789/*uvrY::cam flhDldr::kan flhD-* $tR_2 Ap^r$	This Study
PLB1853	CF7789/*uvrY::cam flhDldr::kan* ΔBS1 ΔBS2 *flhD-* tR_2 Ap^r	This Study
PLB1854	CF7789/*uvrY::cam flhDldr::kan* ΔE *flhD-* tR_2 Ap^r	This Study
PLB1855	CF7789/*uvrY::cam flhDldr::kan* ΔBS1 ΔBS2 ΔE *flhD-* tR_2 Ap^r	This Study
PLB1856	CF7789/*uvrY::cam pyrC::Tn*10 *flhDldr::kan flhD-* tR_2 Ap^r	This Study
PLB1857	CF7789/*uvrY::cam pyrC::Tn*10 *flhDldr::kan* ΔBS1 ΔBS2 *flhD-*tR_2 Ap^r	This Study
PLB1858	CF7789/*uvrY::cam pyrC::Tn*10 *flhDldr::kan* ΔE *flhD-* tR_0 Ap^r	This Study
PLB1859	CF7789/*uvrY::cam pyrC::Tn*10 *flhDldr::kan* ΔBS1 ΔBS2 ΔE *flhD-*tR_2 Ap^r	This Study
PLB1860	CF7789/*uvrY::cam rne-1 flhDldr::kan flhD-* tR_2 Ap^r	This Study
PLB1861	CF7789/*uvrY::cam rne-1 flhDldr::kan* ΔBS1 ΔBS2 *flhD-* tR_2 Ap^r	This Study
PLB1862	CF7789/*uvrY::cam rne-1 flhDldr::kan* ΔE *flhD-* tR_2 Ap^r	This Study
PLB1863	CF7789/*uvrY::rne-1 flhDldr::kan* ΔBS1 ΔBS2 Δ E *flhD-* tR_2 Ap^r	This Study
SK4390	*thyA715 rph-1 rppH::kan*	Mohanty and Kushner, 2010
SK5664	*pyrC::Tn*10 Tc^r	Arraiano *et al*, 1988
SK5665	*rne-1*	Babitzke and Kushner, 1991
SK6632	*thyA715 rnb-500 pnp-200* Cm^r	Yancey and Kushner, 1990
SK6640	*thyA715 rnb-500 pnp-200 rne-1* Cm^r	Yancey and Kushner, 1990
TRCF7789	CF7789/*csrA::kan*	Wei *et al*, 2001
UYCF7789	CF7789/*uvrY::cam*	Suzuki *et al*, 2002

[a] All *flhD'-'lacZ* fusions and truncated promoter-leader regions were integrated into the λ *att* site via the CRIM system (Haldimann and Wanner, 2001). *flhDldr::kan* indicates that the chromosomal *flhDC* leader (−238 to +43 with respect to the start of *flhD* translation) was deleted. ΔBS1 corresponds to a deletion of G7, G8 and A9 from CsrA binding site 1, while ΔBS2 corresponds to a deletion of G50, G51 and A52 from CsrA binding site 2. The ΔBS1 BS2 fusion has all six of these nucleotides deleted. ΔE corresponds to a deletion of several RNase E cleavage sites between +97 to +122 of the *flhDC* leader. tR_2 is an intrinsic terminator from bacteriophage λ.